Electronic Supplementary Material (ESI) for Environmental Science: Nano.

Supporting Information

Different Sulfidized Procedures and Sulfur Precursors Alter the Bacterial Toxicity of Sulfidized Nanoscale Zero-Valent Iron by Affecting the Physicochemical Properties

Haoxuan Zhang[a,b], Long Li[a,b*], Haoran Dong[a,b,*], Shuangjie Xiao[a,b], Junmin Deng[a,b], Daofen Huang[a,b], Junyang Xiao[a,b].

[a]College of Environmental Science and Engineering, Hunan University, Changsha, Hunan 410082, China

[b]Key Laboratory of Environmental Biology and Pollution Control (Hunan University), Ministry of Education, Changsha, Hunan 410082, China

*Corresponding author at:

College of Environmental Science and Engineering, Hunan University, Changsha, Hunan 410082, China.

E-mail address: dongh@hnu.edu.cn (H. Dong); 978751428@qq.com (L. Li)

Text S1. Measure the concentration of total iron and Fe^{2+}

The solution required for the 1,10-phenanthroline colorimetric method was prepared. Firstly, 0.2 g of phenanthroline was dissolved into 100 mL of deionized water. Secondly, 50 mL of acetic acid was volume-fixed with deionized water to 200 mL and adjusted to pH 4.1 with sodium hydroxide. The above two solutions were mixed and recorded as "A" placed at 4 °C away from light. Weighed 10 g of hydroxylamine hydrochloride and dissolved to 100 mL, kept at 4 °C away from light as "B." After preparation, the experiment was started formally, as in the toxicity test, 47 mL of sterile water, 0.5 mL of E. *coli* solution, 2.5 mL of well-dispersed material were added to the reaction flask in turn. At 0, 5, 15, 30, 45, and 60 min of reaction, 1 mL of sample was filtered through 0.22 μm filter membrane, then 500 μL of "A" was added and diluted to a total volume of 5 mL to measure the Fe^{2+} concentration in the solution by UV spectrophotometer at 510 nm. To measure total iron, 1 mL of sample (filtered through a 0.22 μm membrane), 500 μL of "A," and 200 μL of "B" was added in sequence and then diluted to 5 mL with deionized water. The measured results were taken into the standard curve made in advance with $FeSO_4 \cdot 6H_20$ to calculate the actual concentration of Fe^{2+} and total iron.

Text S2. Measurement of intracellular ROS using DCFH-DA as a fluorescent probe

Anhydrous DMSO was used to dissolve DCFH-DA to form a 10 mM stock solution and stored at -20 °C. At 60 min, 1 mL of the sample was added to 2.5 μL of the stock solution and placed at 37 °C for 60 min. After centrifugation at 8000 rpm for 10 min, the supernatant was poured off and then washed in 1 mL of 0.85% saline twice. The extracellular material was cleaned, and 200 μL of saline was added and vortexed well. Take 200 μL of the solution and drop it into a brown 96-well plate ready for measurement. Protection from light is required during the experiment.

Text S3. Reactive Oxygen Species (ROS) quenching experiments

The •OH was quenched with 10 mM IPA, H_2O_2 with 100 mg/L CAT, and $•O^{2-}$ with 10 mM TEMPO. The specific experimental operation was approximately like the toxicity experiment, which mainly needed to add a certain volume or weight of quenching agent after the addition of E. *coli*. The Erlenmeyer flask was then shaken at 20 °C,250 rpm for 5 min until the quencher was well mixed. After that, 2.5 mL of well-dispersed material was added to start the reaction. At 60 min, 0.5 mL of the sample was diluted to the appropriate concentration. Take 0.1 mL of the dilution to coat evenly on EMB agar plates solid medium by the spread plate method and count the colonies after 24 h incubation at 37 °C.

Text S4. Measurement of ·OH concentration by HPLC

The change of •OH concentration in the system with time was detected by high-performance liquid chromatography (HPLC) using the benzoic acid (BA) method. The BA method requires the advanced configuration of BA solution with a concentration of 0.4 g/L. On this basis, the experiment was carried out by sequentially adding E. *coli* solution and materials. At 0, 5, 15, 30, 45, and 60 min, 1 mL samples were filtered by 0.22 μm filter and then detected by HPLC. The measurement results were brought into the standard curve made in advance with p-hydroxybenzoic acid (PHBA) to get the exact •OH concentration. The HPLC was set up with the mobile phase ratio of acetonitrile: 6 M phosphoric acid = 40: 60; the flow rate was 0.8 mL/min; the detection wavelength was 256 nm; the temperature was at 30 °C; the residence time was 2.5 min.

Text S5. Measurement of MDA by Thiobarbituric acid method

The 10% solution of trifluoroacetic acid (TCA) and 0.6% Thiobarbituric acid (TBA) solution were prepared in advance. Experiments were performed by sequentially adding E. *coli* and material. 30 mL samples were taken at 60 min and centrifuged at 8500 rpm for 10 min with the supernatant discarded. 2 mL of TCA solution was added to each sample, vortexed well, and left at 25 °C for 1 h. Subsequently, 1 mL of TBA solution was added to the samples and then placed in boiling water for 30 min, and later placed on ice for rapid cooling. Finally, centrifuge and withdraw 200 μL of supernatant to a 96-well plate. The OD was measured at 532 nm, 600 nm, and 450 nm using an enzyme standard. The MDA concentration is calculated according to the following formula.

$$MDA(\mu M) = \frac{[6.45 * (OD_{532} - OD_{600}) - 0.56 * OD_{450}] * reaction\ volume}{sample\ volume}$$

Text S6. Reaction mechanism for the generation of S-NZVI with different sulfur precursors and procedures

Different sulfur precursors and procedures influence the mechanism of generating S-NZVI(Garcia et al. 2021, Han and Yan 2016, Xu et al. 2019). When Na_2S is the sulfur precursor, it mainly relies on the corrosion of Fe(0) or iron oxide to form FeS (eqs 1-5)(Li et al. 2017, Rajajayavel and Ghoshal 2015). $S_2O_4^{2-}$ will hydrolyze to form thiosulfate and sulfite in an acidic environment (eqs 6-7)(Han and Yan 2016, Kim et al. 2011a) but can hydrolyze to sulfite and sulfide under alkaline conditions (eq 8)(Xiao et al. 2022). $S_2O_3^{2-}$ produces S^0 and SO_3^{2-} under acidic conditions, SO_4^{2-} and S^{2-} under alkaline ones (eqs 9-10)(Xiao et al. 2022). The S^0 can be directly reacted with Fe(0) to produce FeS (eq 11)(Han and Yan 2016). In the one-step method, FeS and Fe(0) will be simultaneously generated(Li et al. 2017). That is, the material is almost uniformly sulfided from inside to outside, thus affecting the internal structure and surface of the materials(Kim et al. 2011a, Su et al. 2018). Furthermore, the pH of the one-step synthesis system will gradually become alkaline with the addition of the reducing agent from acidic(Su et al. 2015, Su et al. 2018), so the hydrolysis of the sulfur precursors will be more complicated (especially $S_2O_4^{2-}$ and $S_2O_3^{2-}$). The two-step method mainly corrodes the surface Fe(0) and iron oxide of NZVI(Brumovský et al. 2020), and the pH of the system is mainly neutral when the vulcanizing agent is added, so the system is relatively simple. To gain a clearer understanding of how the sulfur precursors and procedures affect the material properties, a series of characterizations were performed on six materials.

$$Fe(0) + H_2O \rightarrow Fe(OH)_2 + H_2 \quad (1)$$

$$Fe(OH)_2 \leftrightarrow Fe^{2+} + 2OH^- \quad (2)$$

$$S^{2-} + H_2O \rightarrow HS^- + OH^- \quad (3)$$

$$Fe^{2+} + 2HS^- \rightarrow FeS + H_2S \quad (4)$$

$$2FeS + 2H^+ \rightarrow FeS_2 + Fe^{2+} + H_2 \quad (5)$$

$$2S_2O_4^{2-} + H_2O \rightarrow 2HSO_3^- + S_2O_3^{2-} \quad (6)$$

$$S_2O_4^{2-} + S_2O_3^{2-} + 2H_2O \rightarrow HS^- + 3HSO_3^- \quad (7)$$

$$3S_2O_4^{2-} + OH^- \rightarrow S^{2-} + 5SO_3^{2-} + 3H_2O \quad (8)$$

$$S_2O_3^{2-} \rightarrow S^0 + SO_3^{2-} \quad (9)$$

$$S_2O_3^{2-} + 2OH^- \rightarrow SO_4^{2-} + S^{2-} + H_20 \quad (10)$$

$$Fe(0) + S^0 \rightarrow FeS \quad (11)$$

Text S7. The Two Processes of the Fenton Reaction

During the first phase, Fe^{2+} dissolved by S-NZVI reacts with hydrogen peroxide in the system (eqs 12-15) (Kim et al. 2011b, Kim et al. 2010, Lei et al. 2018), resulting in the production of ROS such as superoxide radicals ($\bullet O^{2-}$), hydrogen peroxide (H_2O_2) and hydroxyl radicals (•OH). The ROS causes oxidative stress, leading to the death of E. *coli*. During the second phase of S-NZVI, a passivation layer is produced, causing the Fe^{2+} dissolution rate to slow down and the generation of ROS to decrease. At this time, the Fe^{3+} in the system reacts catalytically with H_2O_2 (eq 16) (Kim et al. 2011b, Kim et al. 2010, Lei et al. 2018), making the second phase of inactivation much slower than the first phase.

$$Fe\ (0) \rightarrow Fe^{2+} + 2\ e^- \quad (12)$$

$$O_2 + e^- \rightarrow \bullet O_2^- \quad (13)$$

$$\bullet O_2^- + e^- + 2\ H^+ = H_2O_2 \quad (14)$$

$$Fe^{2+} + H_2O_2 = Fe^{3+} + \cdot OH + OH^- \quad (15)$$

$$Fe^{3+} + H_2O_2 \rightarrow Fe^{2+} + \bullet O_2^- + 2\ H^+ \quad (16)$$

Table S1. Surface atomic abundances of six kinds of S-NZVIs

	Fe (%)	S (%)	O (%)
S-NZVI$_{one}$-Na_2S	18.56	2.34	49.83
S-NZVI$_{one}$-$Na_2S_2O_4$	18.66	2.38	46.27
S-NZVI$_{one}$-$Na_2S_2O_3$	18.39	1.65	48.12
S-NZVI$_{two}$-Na_2S	20.65	5.82	44.39
S-NZVI$_{two}$-$Na_2S_2O_4$	19.73	2.7	48.96
S-NZVI$_{two}$-$Na_2S_2O_3$	19.22	3.33	47.75

Table S2. Zeta Potentials of six kinds of S-NZVIs

	Na_2S	$Na_2S_2O_4$	$Na_2S_2O_3$
One-step	2.70 ± 1.2 mV	-0.80 ± 0.8 mV	13.23 ± 0.6 mV
Two-step	-0.71 ± 1.1 mV	0.73± 1 mV	2.18 ± 0.6 mV

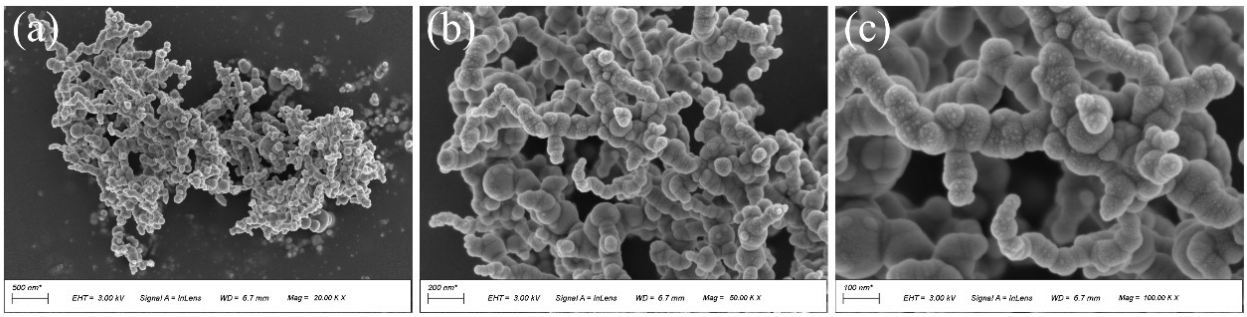

Figure S1. SEM image of NZVI

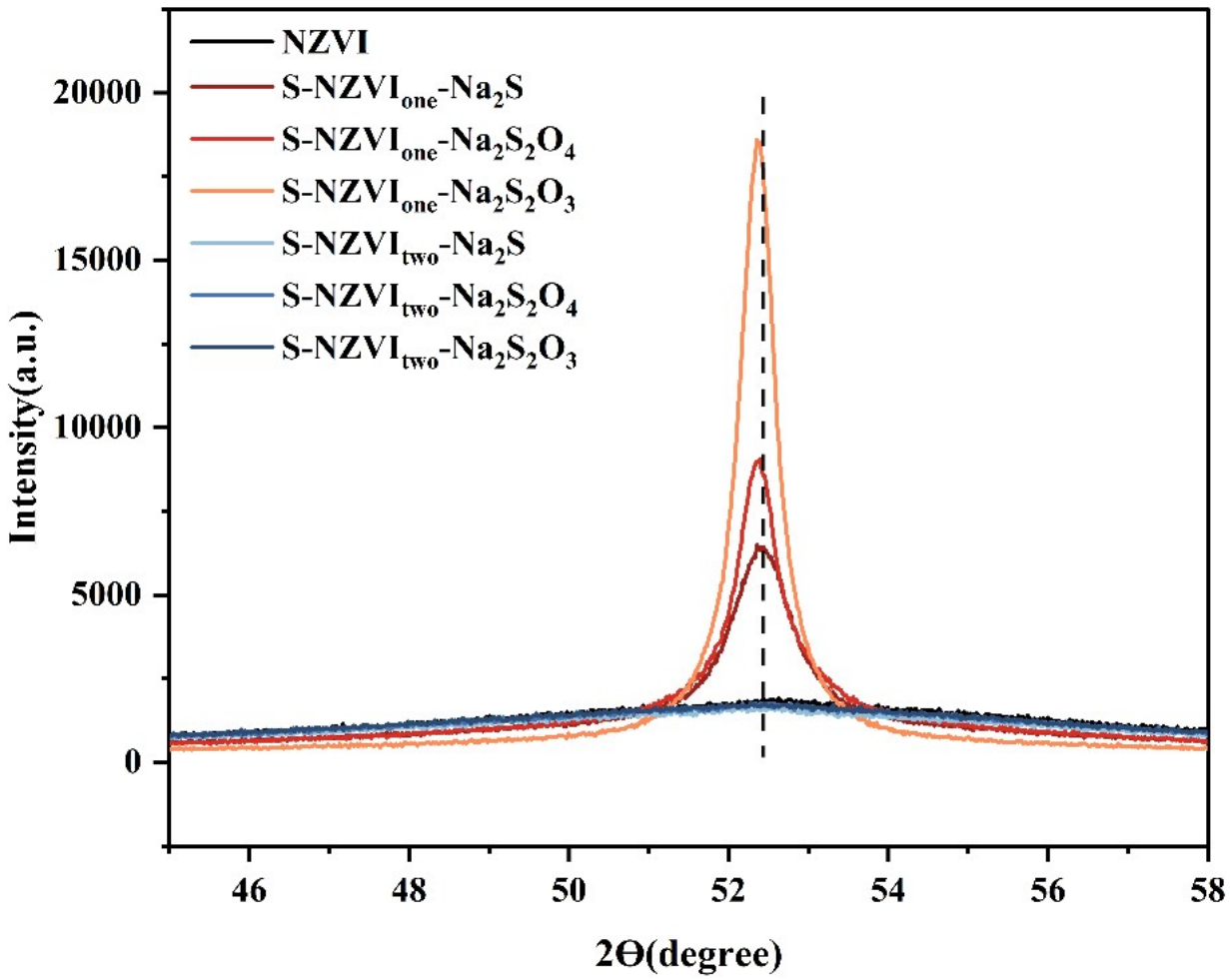

Figure S2. XRD spectra of NZVI and six kinds of S-NZVIs.

Figure S3. Water contact angles of (a) S-NZVI$_{one}$-Na_2S, (b) S-NZVI$_{one}$-$Na_2S_2O_4$, (c) S-NZVI$_{one}$-$Na_2S_2O_3$, (d) S-NZVI$_{two}$-Na_2S, (e) S-NZVI$_{two}$-$Na_2S_2O_4$, (f) S-NZVI$_{two}$-$Na_2S_2O_3$.

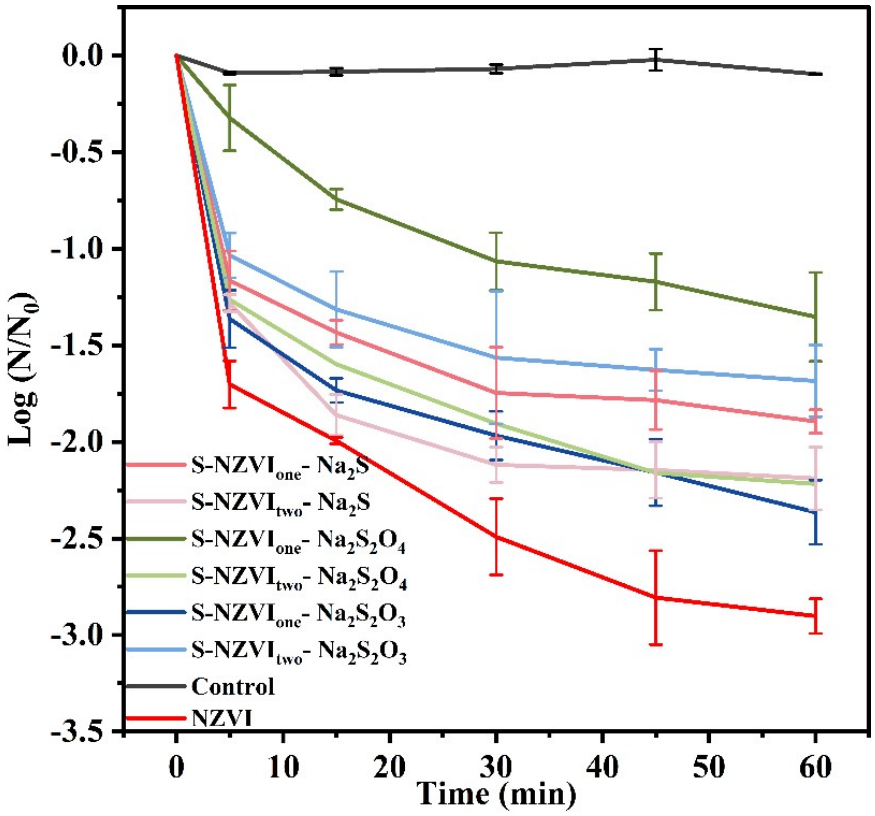

Figure S4. The toxicity of S-NZVI$_{one}$-Na_2S, S-NZVI$_{two}$-Na_2S, S-NZVI$_{one}$-$Na_2S_2O_4$, S-NZVI$_{two}$-$Na_2S_2O_4$, S-NZVI$_{one}$-$Na_2S_2O_3$, S-NZVI$_{two}$-$Na_2S_2O_3$, and NZVI at a concentration of 50 mg/L towards E. *coli* at 0, 5, 15, 30, 45, and 60 min, respectively.

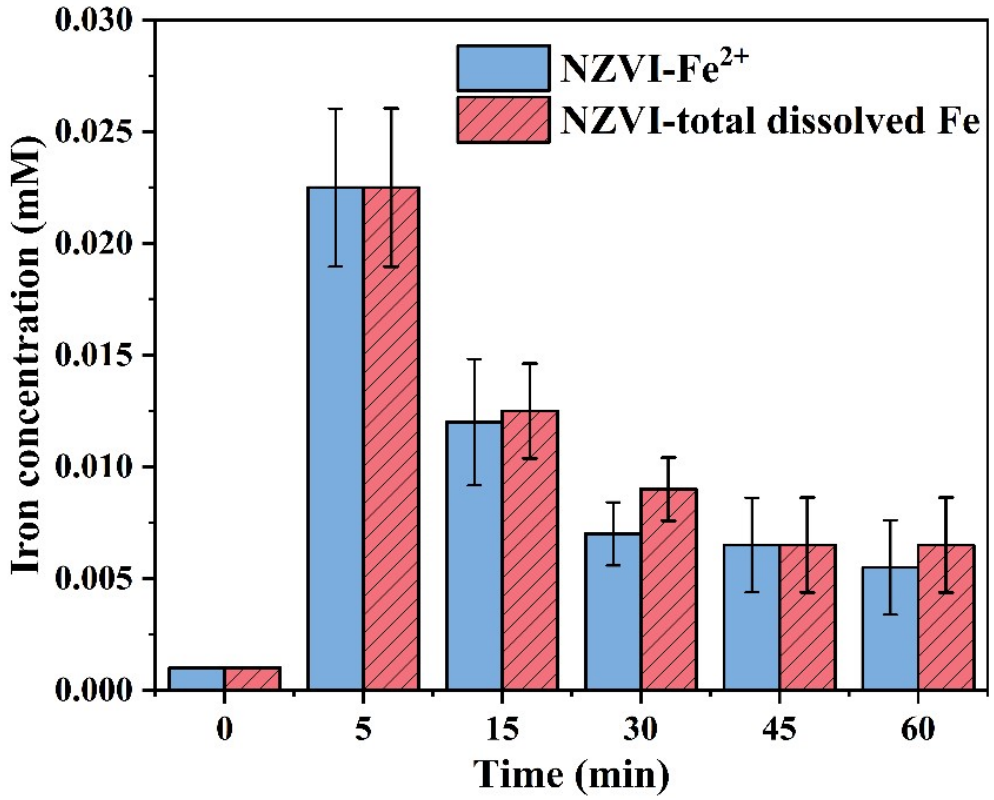

Figure S5. The concentrations of NZVI dissolved Fe^{2+} and total dissolved iron at 0, 5, 15, 30, 45, and 60 min.

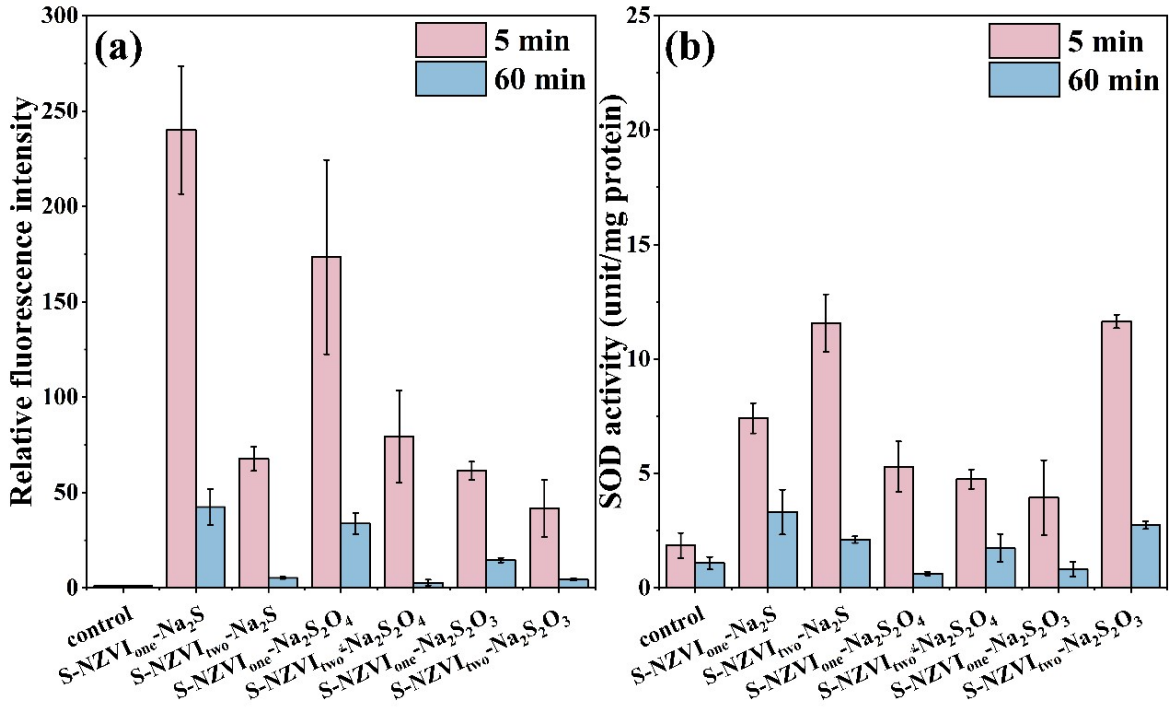

Figure S6. (a) Relative fluorescence values of intracellular ROS at 5min and 60min for six kinds of S-NZVIs. (b) SOD enzyme activity (units/mg protein) at 5min and 60 min for six kinds of S-NZVIs.

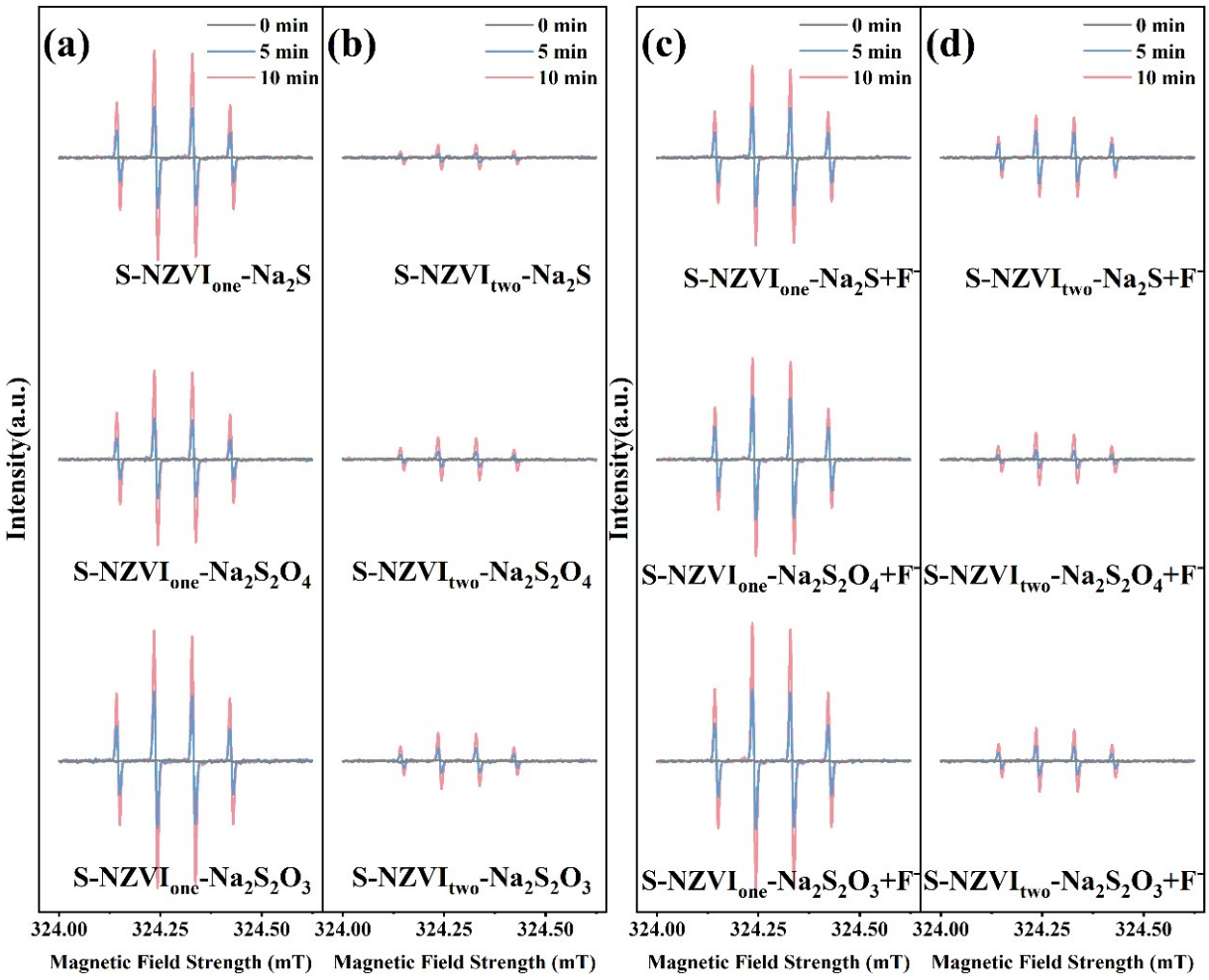

Figure S7. ESR spectra of with DMPO-•OH at 0 min, 5 min, and 10 min for (a) S-NZVI$_{one}$ and (b) S-NZVI$_{two}$. ESR spectra of DMPO-·OH at 0 min, 5 min, and 10 min after the addition of 2 mM of F^- for (c) S-NZVI$_{one}$ and (d) S-NZVI$_{two}$.

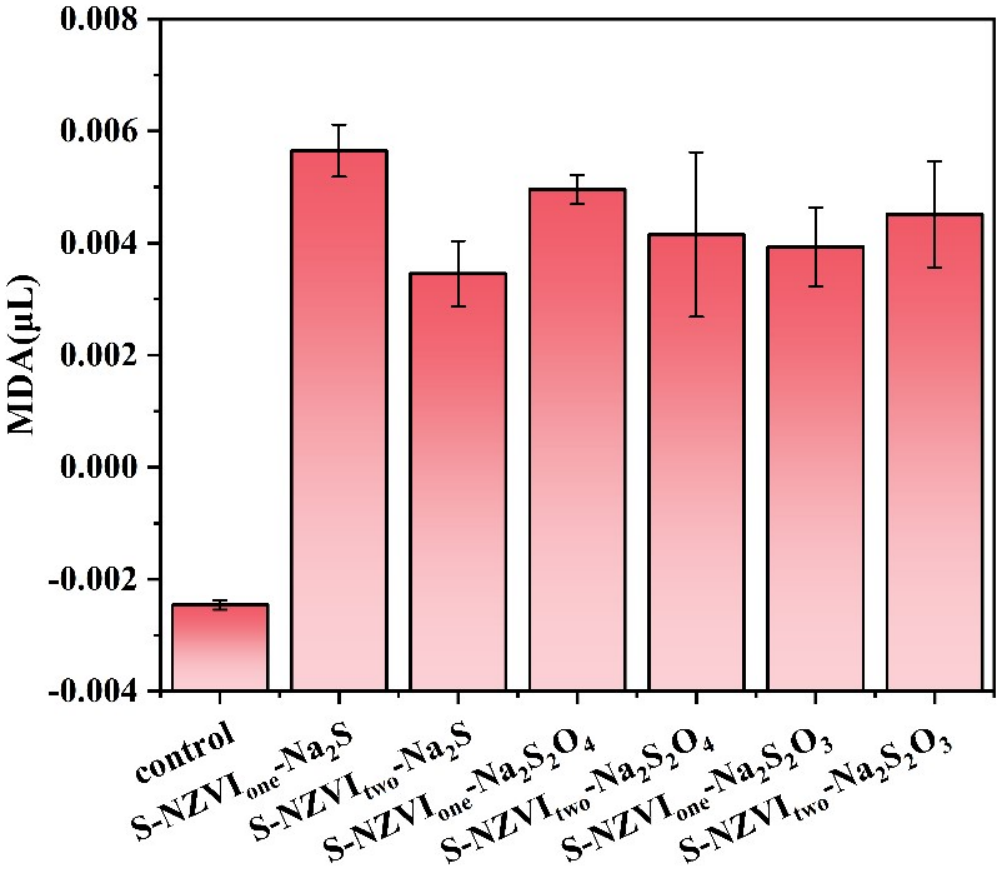

Figure S8. MDA concentrations of the six S-NZVIs treatment systems after 60 minutes of reaction.

References

Brumovský, M., Filip, J., Malina, O., Oborná, J., Sracek, O., Reichenauer, T.G., Andrýsková, P. and Zbořil, R. (2020) Core–Shell Fe/FeS Nanoparticles with Controlled Shell Thickness for Enhanced Trichloroethylene Removal. ACS Applied Materials & Interfaces 12(31), 35424-35434.

Garcia, A.N., Zhang, Y., Ghoshal, S., He, F. and O'Carroll, D.M. (2021) Recent Advances in Sulfidated Zerovalent Iron for Contaminant Transformation. Environmental Science & Technology 55(13), 8464-8483.

Han, Y. and Yan, W. (2016) Reductive Dechlorination of Trichloroethene by Zero-valent Iron Nanoparticles: Reactivity Enhancement through Sulfidation Treatment. Environmental Science & Technology 50(23), 12992-13001.

Kim, E.-J., Kim, J.-H., Azad, A.-M. and Chang, Y.-S. (2011a) Facile Synthesis and Characterization of Fe/FeS Nanoparticles for Environmental Applications. ACS Applied Materials & Interfaces 3(5), 1457-1462.

Kim, J.Y., Lee, C., Love, D.C., Sedlak, D.L., Yoon, J. and Nelson, K.L. (2011b) Inactivation of MS2 Coliphage by Ferrous Ion and Zero-Valent Iron Nanoparticles. Environmental Science & Technology 45(16), 6978-6984.

Kim, J.Y., Lee, C., Sedlak, D.L., Yoon, J. and Nelson, K.L. (2010) Inactivation of MS2 coliphage by Fenton's reagent. Water Research 44(8), 2647-2653.

Lei, C., Sun, Y., Tsang, D.C.W. and Lin, D. (2018) Environmental transformations and ecological effects of iron-based nanoparticles. Environmental Pollution 232, 10-30.

Li, J., Zhang, X., Sun, Y., Liang, L., Pan, B., Zhang, W. and Guan, X. (2017) Advances in Sulfidation of Zerovalent Iron for Water Decontamination. Environmental Science & Technology 51(23), 13533-13544.

Rajajayavel, S.R.C. and Ghoshal, S. (2015) Enhanced reductive dechlorination of trichloroethylene by sulfidated nanoscale zerovalent iron. Water Research 78, 144-153.

Su, Y., Adeleye, A.S., Keller, A.A., Huang, Y., Dai, C., Zhou, X. and Zhang, Y. (2015) Magnetic sulfide-modified nanoscale zerovalent iron (S-nZVI) for dissolved metal ion removal. Water Research 74, 47-57.

Su, Y., Jassby, D., Song, S., Zhou, X., Zhao, H., Filip, J., Petala, E. and Zhang, Y. (2018) Enhanced Oxidative and Adsorptive Removal of Diclofenac in Heterogeneous Fenton-like Reaction with Sulfide Modified Nanoscale Zerovalent Iron. Environmental Science & Technology 52(11), 6466-6475.

Xiao, S.J., Jin, Z.L., Dong, H.R., Xiao, J.Y., Li, Y.J., Li, L., Li, R., Chen, J., Tian, R. and Xie, Q.Q. (2022) A comparative study on the physicochemical properties, reactivity and long-term performance of sulfidized nanoscale zerovalent iron synthesized with different kinds of sulfur precursors and procedures in simulated groundwater. Water Research 212.

Xu, J., Wang, Y., Weng, C., Bai, W.L., Jiao, Y., Kaegi, R. and Lowry, G.V. (2019) Reactivity, Selectivity, and Long-Term Performance of Sulfidized Nanoscale Zerovalent Iron with Different Properties. Environmental Science & Technology

53(10), 5936-5945.